

High-gain imaging electron multiplier

Cite as: Review of Scientific Instruments **44**, 1694 (1973); <https://doi.org/10.1063/1.1686034>
Submitted: 11 July 1972 . Published Online: 06 November 2003

W. B. Colson, J. McPherson, and F. T. King



View Online



Export Citation

ARTICLES YOU MAY BE INTERESTED IN

[Curved-channel microchannel array plates](#)

Review of Scientific Instruments **52**, 1131 (1981); <https://doi.org/10.1063/1.1136749>

[Continuous Channel Electron Multiplier](#)

Review of Scientific Instruments **33**, 761 (1962); <https://doi.org/10.1063/1.1717958>

[Low Energy Charged-Particle Detection Using the Continuous-Channel Electron Multiplier](#)

Review of Scientific Instruments **36**, 375 (1965); <https://doi.org/10.1063/1.1719576>



High-gain imaging electron multiplier

W. B. Colson*, J. McPherson†, and F. T. King‡

Bendix Research Laboratories, Southfield, Michigan 48076

(Received 11 July 1972; and in final form, 12 April 1973)

The chevron-shaped channel electron multiplier is a device which combines the high-gain pulse-counting operation of single channel electron multipliers with the imaging capabilities of microchannel arrays. It produces charge pulses averaging more than 10^7 electrons and these gain magnitudes fall into a quasi-Gaussian distribution with a full width at half-maximum FWHM of approximately 130%. Suppression of ion feedback makes possible both imaging and low noise counting applications over large areas. Dark count rates are typically 1 count/sec cm^2 , and the dynamic range of operation covers 5–6 decades. Active areas over 45 mm diam have been fabricated, with uniform characteristics. Limiting resolution has been measured at 5 line pairs per millimeter. Because of the short length of each channel electron multiplier, the rise time and width of the output charge pulses are extremely short; large signal pulses have been detected with rise times as short as 400 psec.

Channel electron multipliers¹ have been used extensively as detectors of high energy photons and charged particles. They have been used in phototubes, laboratory vacuum chambers, and space environments for detection of charged particles, metastable atoms, and energetic photons.^{2,3} The suppression of ion feedback, a major consideration when these devices are used in high-gain applications, has been accomplished by curving the channels (in a variety of configurations) so as to discriminate against lengthy ion trajectories while allowing for the shorter electron trajectories inside the channel. The flexibility in geometrical design necessary to achieve this aim is accomplished by using glasses specially formulated to have suitable characteristics, i.e., resistivity and secondary emission. Single channels typically have output pulses containing about 10^8 electrons and, because of space-charge saturation on each pulse, can be operated in the pulse mode in connection

with standard event-counting instruments. This means that all input events are represented by output charge pulses whose magnitudes fall into a narrow, quasi-Gaussian distribution.⁴

A parallel development with single channel electron multipliers, the fabrication of the microchannel array, utilizes the same advantageous properties of glasses.^{5,6} The microchannel array consists of many parallel tubes having essentially identical but independent electrical properties, fused together so as to provide an area capable of electron multiplication. Because each channel operates independently, such an array can resolve simultaneous events that are spatially separated by distances on the order of the channel size. The channel size can be as small as $\sim 10 \mu$. A scanning electron microscope picture of 50μ diam channels is shown in Fig. 1. Each channel wall is constructed from three layers of different glass. The surface layer is semiconducting and determines the secondary emitting properties of the channel. The second layer provides the structure of each microchannel and the third innermost layer fuses channels together. The channels in the array are not curved because of the nature of the fabrication process, and high electron gains exceeding 10^4 cannot be achieved without serious ion feedback. Useful output charge pulses must therefore be limited in magnitude.

The microchannel array electron multiplier explored here is an amalgam of single channel and microchannel array technology which juxtaposes two suitably cut and oriented microchannel arrays.⁷ A cutaway schematic of the two

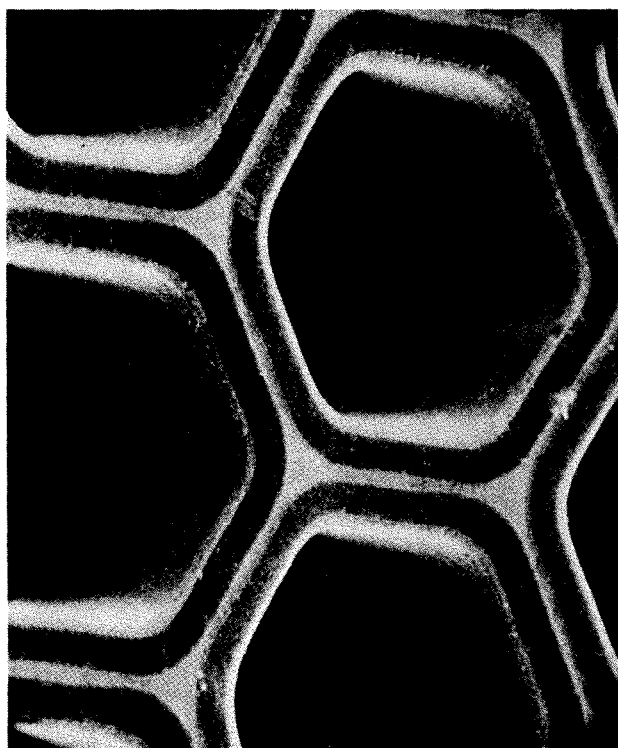


FIG. 1. Microchannel structure.

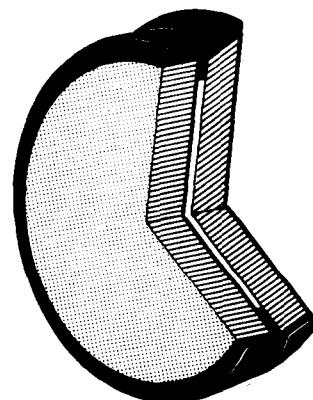


FIG. 2. Electron multiplier structure.

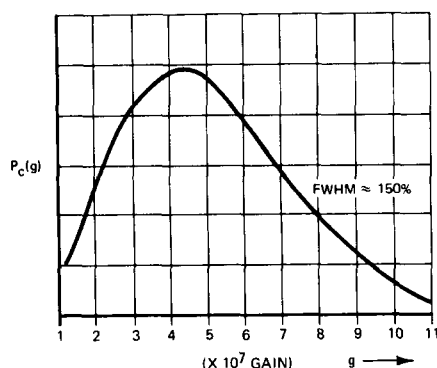


FIG. 3. Pulse magnitude distribution.

arrays includes a sharp bend at the junction of the arrays (see Fig. 2). Because the resultant shape of an effective channel is bent, the device has been referred to as a chevron-shaped electron multiplier (CSEM). This orientation effectively bends the channel through which electrons and ions pass, thereby suppressing ion feedback just as with single channels. Suppression of ion feedback in turn allows high gains and operation in the pulse-saturated mode. The device is then suitable for particle counting applications; in addition, it offers position sensitivity. Particle counting with a spatial resolution of 5 line pairs per millimeter over large areas has been demonstrated. This spatial resolution was obtained by using an Air Force resolution target over the input of the device and imaging the output pattern on a phosphor screen. It is implicit in this test that dark noise is small when used as an imaging device. The character of the imaging operation is similar to that of Spiraltron channel arrays.⁸ Compared to the Spiraltron array, this composite array (CSEM) offers improved spatial resolution, larger detection area, and reduced cost.

Typical performance characteristics of several operating devices are given in Table I. The gain is approximately that which would be expected from operating two microchannel arrays in series. The pulse magnitude distribution, however, is quasi-Gaussian and shaped like that of a single curved channel; whereas typical microchannel arrays have exponential distributions. The pulse magnitude distribution is wider than that usually achieved in single channels, being on the average 130% FWHM at the operating voltage compared to about 50% for single channels (See Fig. 3). Explanation of this requires a closer look at the electron multiplication process.

A charge pulse initiated in the first section of the CSEM will contain about 10^3 electrons with a quasiexponential distribution upon exiting that section. This charge will

flow into N channels of the second section. If N is not too large, then each of the N channels will receive enough charge to produce a space-charge saturated output pulse; this is desirable. It is also desirable that N is not large, so as to preserve as much information as possible concerning the position of the initial event, e.g., higher resolution. Assuming N is small enough, then each of the N channels produces a charge pulse whose magnitude is described by the distribution of a single microchannel which should be approximately

$$p_s(g)dg \sim \exp[-(g-\bar{g})^2/\sigma^2]dg, \quad (1)$$

where \bar{g} = average gain $\approx 5 \times 10^6$, σ = (mean deviation from \bar{g}) = $0.6\bar{g}$, g = gain, e.g., number of electrons in a charge pulse, and $p_s(g)$ = probability of gain g from a single microchannel occurring between gains g and $g+dg$. We have not measured g or σ directly, but have estimated values from extrapolation of single channel data.⁴ It is important to note that we are assuming that each of the N channels operates nearly identically and independently.

In addition to the statistical process, $p_s(g)$, for each of the N saturated microchannels in the second section, there is a statistical variation in N . For a given site there is an average \bar{N} over many charge pulses, and this \bar{N} may vary from site to site. We know that \bar{N} can be made a function of position by choosing appropriate spacings and electric field between the sections.

When \bar{N} becomes a function of position, we can observe a moiré pattern of the output current focused onto a phosphor screen. We have been able to find a spacing and field strength between the sections such that image resolution is optimized with no observable nonuniformities due to variation in \bar{N} from site to site.

When operating at these optimized parameters, we find that the average CSEM gain is about three times that expected for a single microchannel; e.g., $3\bar{g} \approx 1.5 \times 10^7$. Also the resolution elements are about twice the diameter of a single microchannel. We observed resolution elements on the order of $\sim 100 \mu$ in size (5 line pairs per millimeter) with 50μ channels. This indicates that $\bar{N} \approx 3$ is constant over the active area of the array of the microchannels. We have made each image site operate nearly identically but there is still a variation in N at each site from charge pulse to charge pulse. This we feel leads to the widening in the pulse magnitude distribution. The operation of the total device may be described by an expression of the form

$$P_c(g)dg \sim \sum_N A_N \exp[-(g-N\bar{g})^2/N\sigma^2]dg, \quad (2)$$

where A_N is a weighting parameter describing how often the first section excites N channels in the second section, $P_c(g)$ = probability of gain g from a CSEM occurring between gains g and $g+dg$. From our observations, we expect that A_N is maximum for $N=3$.

The process described by $P_c(g)$ is very much like another Channeltron electron multiplier device, the preamplified Spiraltron electron multiplier.⁹ In this case, a straight, low-gain single channel is used to simultaneously excite all six channels of the following Spiraltron element. The device is

TABLE I. Operating characteristics.

Code #	Active diameter (mm)	Applied voltage	Gain ($\times 10^7$)	FWHM of gain distribution (%)	Dark counts (sec/cm ²)
214-23-5, 2	45	2000	1	130	0.2
209-21-6, 2	45	3000	1.75	135	1
209-22-13, 19	23	2240	1.3	115	0.3
209-22-12, 18	23	2400	1.2	155	0.6
209-24-15, 11	15	2080	1	145	1.0
212-20-06, 03	15	2160	1.7	135	0.8

designed so that essentially there is only one term, $N=6$, in the sum (2). The preamplified Spiraltron has a correspondingly narrower pulse magnitude distribution than the multiplier described in this paper.

Additional advantages can be realized in a chevron-shaped device, such as good temporal resolution and a pulse width of less than 1 nsec with a rise time of less than 0.5 nsec. The transit time for a charge pulse is estimated at less than 1 nsec; the transit time jitter, at less than 100 psec. This device was used in a fast photomultiplier tube; it gave results consistent with the above estimates.¹⁰ In this tube a fast pulse of photons from a high pressure mercury arc was detected as a large charge pulse having a rise time of about 400 psec (see Fig. 4). Since the CSEM is much faster than conventional-type multipliers, its application in fast photomultipliers is expected to be one of its important uses.

The low dark count rate of the device (1 count/sec cm² in a demountable vacuum system) permits its use in scientific experiments where previously only single channel detectors had been feasible. This low dark count rate is essentially independent of applied voltage over the normal operating range of several hundred volts. Operated in the pulse counting mode, it can be used with a multianode collector for direct analog-to-digital conversion readout (sensing) of multiple wavelengths in the vacuum uv region. Arrays with large active area up to 17 cm² have been made, with little variation in characteristics over the area. We estimate the plate uniformity at <5% deviation from the average except at points arranged in a regular pattern called "webbing." Webbing in chevron devices is typical for microchannel plate electron multipliers. Studies show that there are no fundamental problems with still larger sizes. The chevron-type array is also a nearly ideal detector for an energy-dispersion electron experiment; it is being applied in this way as the output element in a very sensitive electron spectroscopy chemical analysis ESCA instrument. The emission of exoelectrons from surfaces has been imaged using this array.¹¹

For all channel electron multipliers, the maximum count rate is determined by the strip resistance of the channels.¹² Therefore, the maximum long-term counting rate for the new device operating in the pulse mode is about 10⁶ counts/sec cm² of active area. The magnitude of each pulse will be somewhat depressed at this counting rate, but charge pulses are still large enough to be distinct and useful. At count rates less than 10⁵ counts/sec cm², all charge pulses are at full magnitude and no gain depression is observed. These

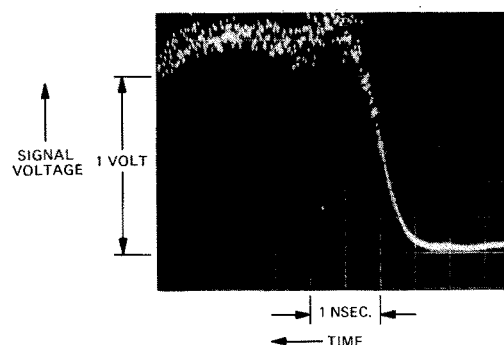


FIG. 4. Pulse rise time.

data, when compared with the low dark noise of the device, indicate that it has a dynamic range of 10⁵–10⁶ in the counting mode.

Chevron-shaped channel electron multipliers can be made to have high resolution capabilities by using small microchannels. The feasibility of high resolution was established using 13 μ microchannels. Resolution of 14 line pairs per millimeter was observed. The average gain was decreased by a factor of about three because the level of space-charge saturation is a linear function of absolute channel size.⁴ Other operating characteristics are very close to those listed in Table I.

We wish to acknowledge helpful discussions with W. G. Wolber and G. W. Goodrich.

*Present address: Dept. of Physics, Stanford University, Stanford, Calif. 94305.

†Present address: 23920 E. Leboast Ave., Novi, Mich. 48050.

‡Present address: 24025 S.W. Tualatin Valley, Hillsboro, Oregon 97123.

¹G. W. Goodrich and W. C. Wiley, *Rev. Sci. Instrum.* **33**, 761 (1962).

²G. W. Goodrich *et al.*, *Proc. 1967 NAECON* 1967.

³M. C. Johnson, *Rev. Sci. Instrum.* **40**, 311 (1969).

⁴K. Schmidt and C. F. Hendee, *IEEE Trans. Nucl. Sci.* **NS-13** (3), 100 (1966).

⁵C. E. Catchpole, "Electron Image Amplification using Microchannel Plates," presented at Optical Society of America Spring Meeting, Philadelphia, Pa., 1970.

⁶G. Eschard and R. Polaert, *Philips Tech. Rev.* **30**, 252 (1969).

⁷G. W. Goodrich, U.S. Patent No. 3,374,380.

⁸T. A. Somer and P. W. Graves, *IEEE Trans. Nucl. Sci.* **NS-16** (1), 376 (1969).

⁹W. G. Wolber, B. D. Klettke, and P. W. Graves, *Rev. Sci. Instrum.* **41**, 724 (1970).

¹⁰Private Communication, B. Leskovar, Lawrence Radiation Laboratory, University of California, Berkeley. Measurements on Bendix fast photomultiplier tube incorporating CSEM.

¹¹P. Braunlich, *J. Appl. Phys.* **42**, 496 (1971).

¹²B. D. Klettke, W. L. Wilcock, R. K. Mueller, and W. G. Wolber, *Appl. Phys. Lett.* **16**, 421 (1970).